Journal of Materials and Engineering Structures

Research Paper

Sorption mechanism of copper ions on synthetic and natural dentine hydroxyapatites

Farida Fernane [a],*, Saliha Boudia [a], Ahmad B. Albadarin [b], Farid Aiouache [c],

[a] *Laboratoire Ressources Naturelles – Mouloud Mammeri University, BP N°17 RP, 15000 Tizi-Ouzou, Algeria*

[b] *Bernal Institute, Department of Chemical and Environmental Sciences, University of Limerick, Ireland*

[c] *Engineering department – Lancaster University, LA1 4YW, Lancaster, UK*

ARTICLE INFO

ABSTRACT

Removal of copper ions from aqueous solutions on synthetic and dentine waste hydroxyapatites (HAP) was investigated in batch sorption experiments. Kinetics of sorption followed a pseudo-first order model. Steady-state data show agreement with the Sips isotherm compared with Freundlich and Langmuir models. The higher surface area and carbonated nature of synthetic hydroxyapatite were not sufficient to reach higher sorption capacity than natural one. Ion-exchange and precipitation contributed on removal of Copper despite level ionization of hydroxyapatites. Proton and metal exchanges with copper ions contributed to process of sorption with prevalence of proton-exchange at low copper ion concentrations. High temperatures promoted the removal efficiency of Cu(II) onto the natural and synthesised hydroxyapatites. The thermodynamic parameters showed that sorption process was spontaneous, endothermic and associated entropy at the solid/solution interface increased at high temperatures.

1 Introduction

The removal of metals from wastewater is a topic of growing concern, owing to dramatic consequences on human health and clean water supply. Life cycle of metals, which are identified to be toxic and non-biodegradable such as copper, lead, cadmium, etc.[1], includes collection by microorganisms and further transfer to humans through mainly the food chain [2-6]. Copper in the form of Cu^{2+} ions was found among the major metals that are polluting the environment due to increasing activities of mining and applications to oil, gas and manufacturing industries (e.g. concrete, paper, wood, glass, ceramic products, etc.) [7]. It is not surprising to observe extensive studies on depollution of waste waters by metal removals to meet tightening regulations [8]. Various techniques are used including filtration, adsorption, ion exchange, reverse osmosis and

RESEARCH REVIEW of
Sciences and Technologies

electrocoagulation [8]. Adsorption is generally a competitive process due to its performance, less complexity , accessibility to adsorbents [9]. Adsorbents, particularly those obtained from environmentally friendly resources such as apatites, crop milling, olive stones and sawdust are attracting attention for potential applications, especially to regions of world that use limited mature technologies. [10-13]. Equally with other resources, apatite based materials are suitable media to take off toxic metals from polluted waters [14-20] because they are known to be stable under reducing or oxidizing conditions and available at affordable costs [21]. Apatites are defined by the chemical formula $M_{10}(RO_4)X_2$, where R, M and X are commonly phosphorus, calcium and hydroxide or a halogen ion (i.e. fluorine, chlorine), respectively[14-18]). Calcium hydroxyapatite (HAP) of theoretical formula $Ca_5(PO_4)_3(OH)$ is a bio-ceramic that has seen growth recently due to applications to dentistry and orthopaedic surgery[22]. This material, which is partly soluble in water, was demonstrated to exhibit higher metal removal efficiency than relevant materials such as rocks and fertilizers [20,23, 24]. However the mechanism of retention remains not clear and would be associated with ion-exchange, mass transfer by diffusion and precipitation of formed solids, depending on the operating conditions (i.e. pH, flow dynamics, temperature and solid surface properties), and the reactivity of the substituted HAP [7, 14, 25-29]. Sugiyama et al. [30] suggested two mechanisms relevant to adsorption of divalent metal cations. The first would undergo ion adsorption, diffusion into HAPs pores and release of cations, originally contained inside HAPs pores, by an ion-exchange. The second would involve dissolution of HAPs into the aqueous solution and precipitation or co-precipitation of metal phosphates. Other mechanisms would include sorption-complexation at high pH values and dissolution–precipitation at highly rich-proton values (pH <4) [31-34].

The aim of this study is to investigate ability of natural HAP obtained from waste human crushed teeth to remove Cu (II) from aqueous solutions. The study will therefore look at the mechanism taking place over the uptake and discuss the results by comparing the performance of separation with synthetic HAPs. Moreover, the results would give more understanding of mechanism of mineralisation of teeth and bones, where the content of Cu(II) which was found to be inversely proportional to the content of calcium [35, 36]. Both equilibrium and kinetic sorption models are proposed and relevant mechanisms are discussed.

2   Materials and Methods

2.1 Hydroxyapatite sorbent

The natural Hap (N-HAP) was supplied by a medical dentistry and was part of a selection of extracted human teeth [37]. These teeth were washed with a solution of 10% hydrogen peroxide and sodium hypochloride during 24 hours, and a solution of 1% of nitric acid. The mixture was then dried at 30ºC for24 hours. The teeth were ground by using a ceramic mortar, sieved for a range from 106 to 710μm size and then dried at 60ºC for 8 hours. Such particles were reported to contain nearly 75% HAP minerals [38]. The synthetic HAP (S-HAP) was supplied by Bio-Rad (Bio-Rad®DNA Grade Bio-Gel HTP 130-0420).

The chemical compositions of the both N-HAP and S-HAP were determined by inductively coupled plasma atomic emission spectrometry (ICP/AES (Varian Vista Spectrometer). Scanning electron micrographs (SEM) were made with a Phillips ESEM after gold sputtering of the HAP surfaces.X-ray diffraction analysis was carried out by using a Philips powder diffractometer operating, Cu K alpha radiation (λ=1.5418·10^{-10} m) at 40 KVA and 20 mA, 0.1°step from 2θ = 10 to 70 and one second step time.The specific surface area and porosity distribution of HAP powder were examined byN_2 adsorption measurements which were performed at liquid nitrogen temperature 77 K, using the Brunauer, Emmett and Teller N_2-BET method (Coulter-SA3100 device).

Further characterization by infrared (IR) of the dried powder was carried out by using KBr discs (sample/KBr mass ratio 1:100), Fourier-transform infrared (FTIR) spectrometer (Shimadzu FTIR-8400 S, Japan), a frequency ranging from 500 to 4000 $cm^{-1}$and room temperature.

2.2 Adsorption experiments

The sorption tests experiments were performed by mixing at 120 rpm sorbent (0.5 g) and a solution of 50 mL of cupric nitrate in polyethylene bottles. Concentration of copper solution was varied from 20 to 1000 mg.L^{-1} and shaken. The sorption equilibrium tests were achieved by sampling at time intervals until steady residual values of sorbent were established. The solutions were then filtered and analysed by ICP/AES for Cu and Ca elements. The pH of the solutions was insured to remain

at 4 by measuring acidity of the solution along with the sorption tests. This would avoid hydroxide precipitation of copper at pH higher than 6 and hydroxyapatite dissolution at pH lower than 4 [7, 27 and 28].

3   Results and discussions

3.1 *Hydroxyapatite characterisation*

Table 1 summarizes results of chemical composition and specific surface area of both N-HAP and S-HAP. These results show that the chemical compositions of two HAP are close in spite of the differences noted on the specific surface values and the porous volume.

Table 1: Chemical compositions of both N-HAP and S-HAP.

	Specific surface area $(m^2.g^{-1})$	Pore volume (mL/100g)	Composition
N-HAP	1.50	12.9	$Ca_{8.92}(PO_4)_6(OH)_2$
S-HAP	43.16	19.7	$Ca_{8.89}(PO_4)_6(OH)_2$

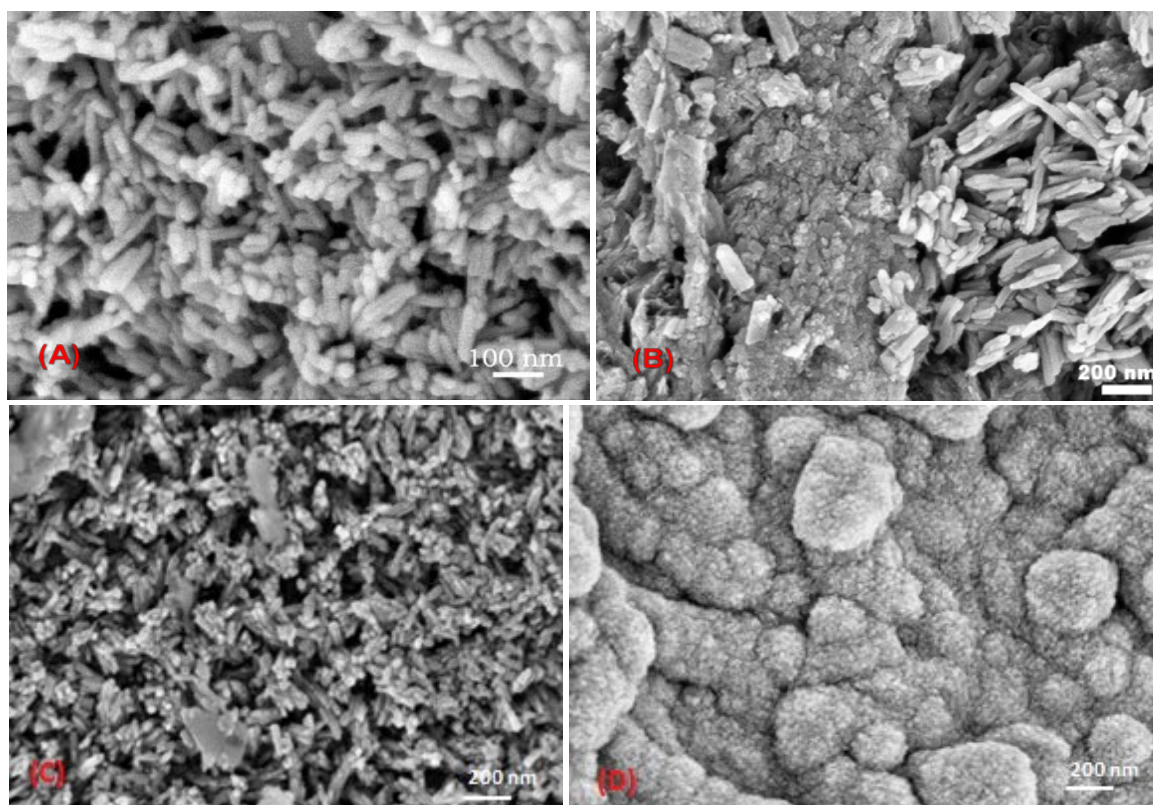Figure 1 illustrates morphology of N-HAP and S-HAP.

Figure 1- SEM view of unloaded S-HAP (A), N- HAP (B), loaded S-HAP(C) and N-HAP (D) after copper sorption

Figure 1(A) shows that S-HAP has morphology of sticks. N-HAP exhibits a more heterogeneous morphology with presence of typical tubule of dentine of micrometer size and regularly separated by an average distance of 8 µm as clearly observed in Figure 1(B).

The SEM descriptions of S-HAP and N-HAP after copper sorption are shown in Figures 1(C) and (D), respectively. It can be seen that at high magnification, the endogenous N-HAP was completely covered with the new formed precipitates including the pores of the tubuli. S-HAP exhibited surfaces of the original crystals which were coated with the formed crystallites, leading to a different morphology of formed precipitates. This was likely driven by the strong presence of

carbonates ions (showed by absorption band at 1430cm^{-1} in Figure 10) as well as the large pores and relatively dense trabecular of N-HAP compared with the micrometre orders crystallites and pores of S-HAP.

From the XRD scans (Figure 2), the S-HAP presented peaks that belong to a crystalline structure, while the N-HAP presented peaks which slightly shifted due to the presence of NaCaPO$_4$. These results confirm our previous finding where N-HAP had shown large pores and relatively dense trabecular and the S-HAP presented micron-sized crystallites of micron-sized pores left after the drying process [37]
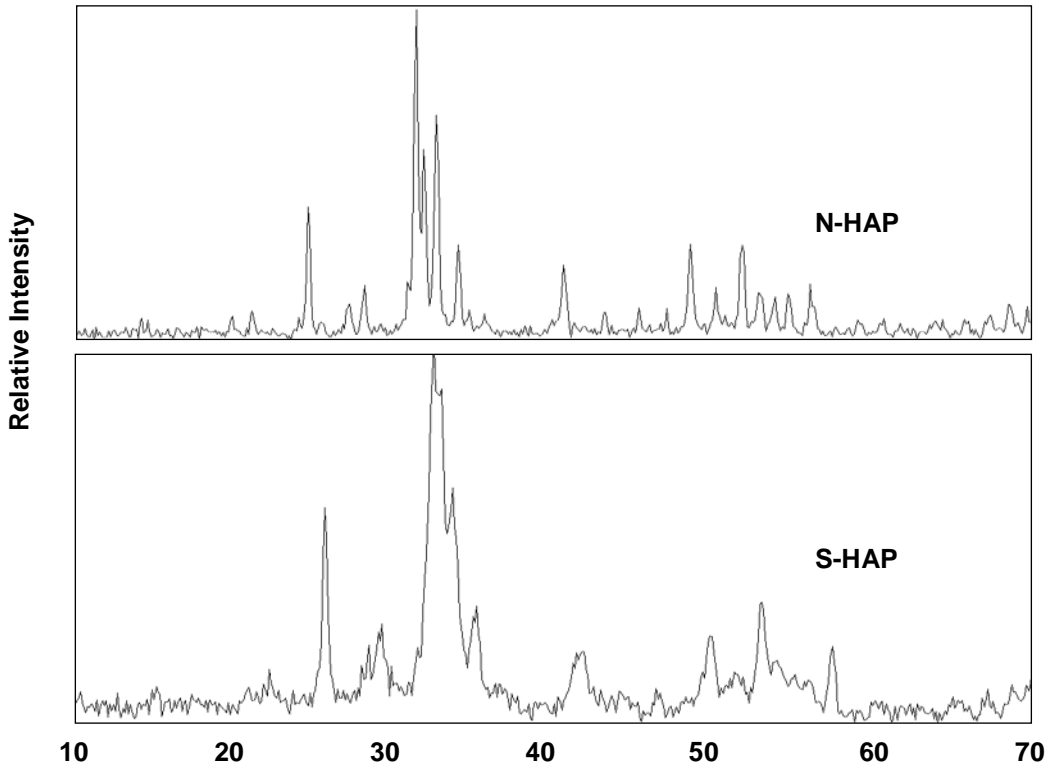

Figure 2: X-ray powder patterns of natural N-HAP and synthetic S-HAP hydroxyapatite

3.2 Kinetic modelling

Figure 3 shows variation of sorption kinetic at 20°C, pH4, solid/liquid ratio of 10 g/L and initial Cu(II) concentrations of 500 and 1000 ppm. Adsorption rates are seen to be relatively fast for the first 90 minutes before reaching equilibrium at approximately 120 and 200 minutes for 500 and 1000ppm, respectively. Such high rates at the start may indicate a strong surface complexation during the adsorption process [39]. The figure 3 shows that the adsorption rate (dq/dt) decreases with time until it gradually approaches the equilibrium state due to the continuous decrease in the driving force (qe $-q$t).

The plots in Figure 3 also demonstrate that the adsorbate uptake, q, increases with increasing the initial concentration [40]. Copper ions removal onto N-HAP rate was relatively rapid when compared with S-HAP as the former was able to adsorb 30 mg/g of Cu within the 100 minutes while S-HAP achieved 28 mg/g of Cu at C$_o$ = 500ppm. The relatively fast reduction in Cu concentration may indicate a high accessibility to hydroxyl groups and metal exchange.

How close is the temporal adsorption from it's the adsorption is illustrated in Figure 4, where the kinetic profile of fraction of uptake f, f= q/q$_e$, is presented. Unlike the fractional uptake, the time that is needed to reach equilibrium increased with initial concentration.

Conventional kinetic models of pseudo-first order and pseudo-second-order were attempted. These two models would give details on type of mechanism that is taking place. The pseudo-first order model is typically used to describe an adsorption process where the rate is proportional to the number of vacant sites of the sorbent [41, 42], and expressed by equation (Eq. (1)) [43]:

$$q_t = q_e \left(1 - e^{-k_1 t}\right) \qquad (1)$$

Where k_1 (min^{-1}) is the pseudo-first order adsorption rate constant. The pseudo- second order kinetic model expresses complex sorption mechanisms where the rate is not only function of vacant sites but also function of associated processes such as ion-exchange, and expressed by equation (Eq.(2)) [21, 42– 43]:

$$q_t = \frac{k_2 q_e^2}{\left(1 + k_2 q_e t\right)} t \tag{2}$$

Where k_2 (g.mg^{-1}min^{-1}) is the pseudo-second order adsorption rate constant.
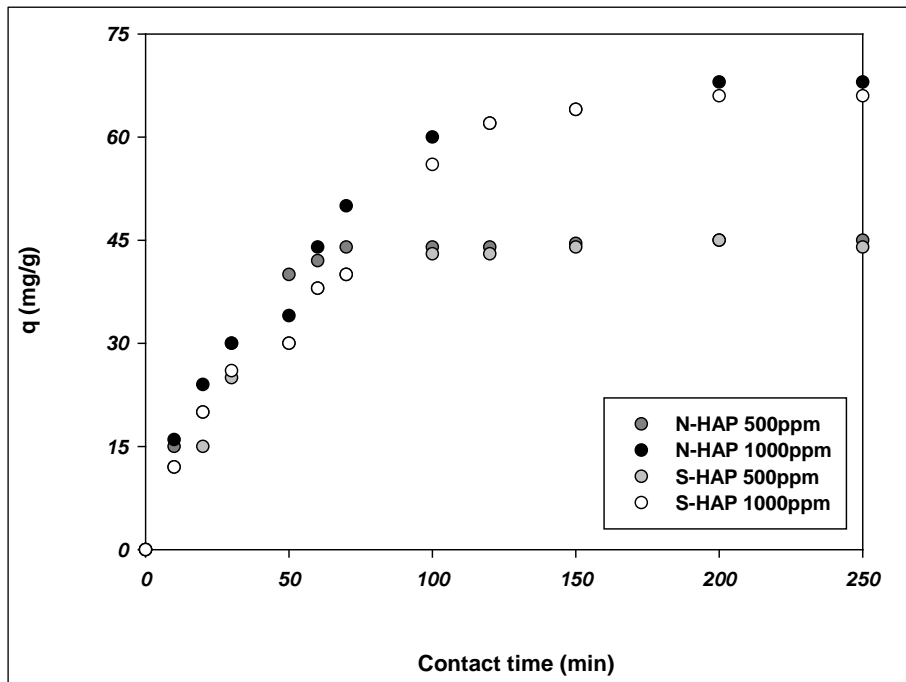

Figure 3: Effect of contact time and initial concentration on copper amount removed per gram of N-HAP and S-HAP (600 rpm, pH = 4 and 20°C).
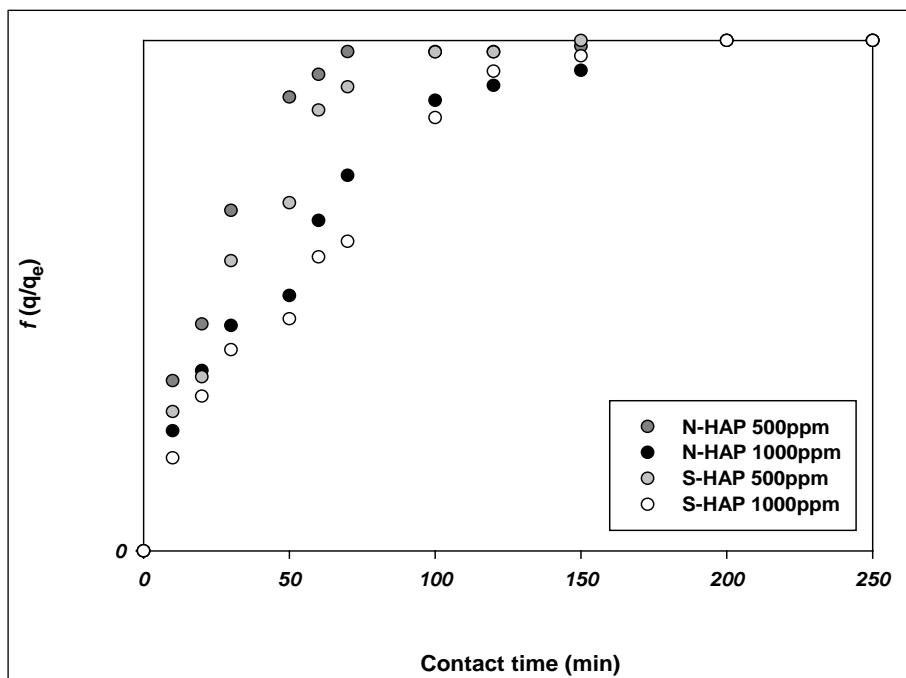

Figure 4: The fractional approach to equilibrium with time for different initial copper concentration at 20°C.

The kinetic data were then fitted to both models and rate constants relevant to the both kinetic models are illustrated in Table 2. Figure 5 shows profiles of both kinetic models along with the experimental data. The pseudo first- order model shows a good agreement with experimental data where the correlation coefficients for the linear plots were higher than 0.98 for all the experimental data, confirming that process of Cu removal was driven by the mechanism of sorption. The results of Table 2 indicate that adsorption capacities ($q_{e,cal}$) from model calculations were close to the experimental ($q_{e,exp}$) for both S-HAP and N-HAP. In addition, relevant activation energy, which was obtained by plotting the Arrhenius model (not shown) relevant to rate constant k_2, was about an averaged value 67.42 kJ/mol, demonstrating a potential impact of mass transfer on the kinetics of adsorption.
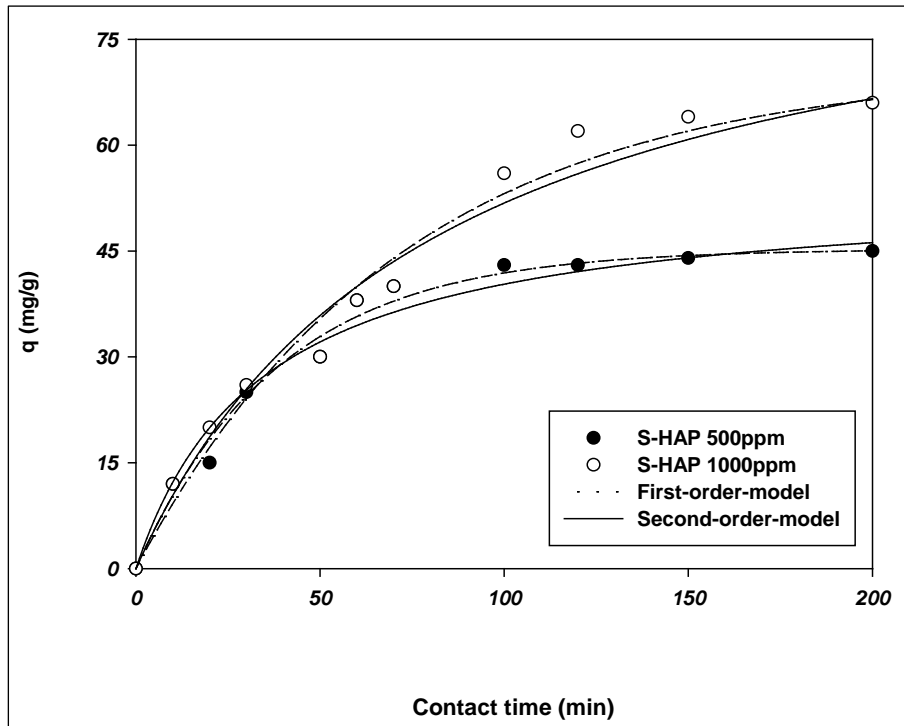

Figure 5: Profiles of the pseudo first-order model and pseudo second-order model.

Table 2: Pseudo first-order, pseudo second-order and Weber model constants and correlation coefficients

	Pseudo first-order model				Pseudo second-order model			Intraparticle diffusion model	
	$q_{e,exp}$	$q_{e,cal}$	k_1	R^2	$q_{e,cal}$	k_2	R^2	k_{diff}	R^2
N-HAP 500ppm	45.13	45.45	0.037	**0.989**	52.09	0.001	0.965	0.084	0.925
N-HAP 1000ppm	68.07	69.40	0.018	**0.984**	86.76	0.0002	0.982	0.015	0.937
S-HAP 500ppm	44.02	45.28	0.026	**0.986**	54.09	0.0005	0.970	0.715	0.915
S-HAP 1000ppm	66.10	70.91	0.014	**0.981**	93.25	0.0001	0.975	0.412	0.907

Where q_e, mg/g; k_1, 1/min; k_2, g/mg min.

3.3 Mass transport effect

The contribution of transport to the overall rate was examined through Weber intraparticle diffusion model [6, 43], which is given by:

$$q_t = k_{diff} \times t^{0.5} \tag{3}$$

Where k_{diff} (mg/g min$^{0.5}$) is the intraparticle diffusion rate constant. The Weber model determines relevance of internal mass transport only, mainly by diffusion inside the pores of HAP. or diffusion through the external boundary layer (surface film between the solid and liquid phases) [6, 43].The plot of q_t versus $t^{0.5}$ (Figure 6 (only plots for C_o = 20 and 100mg/L are

shown)) illustrates that Weber model did not fit well experimental data and the plots do not pass through the origin, indicating that intraparticle diffusion was not the rate controlling step but two types of mechanisms are operating in the removal of Cu(II). The plots show two straight lines of different slopes. The first line corresponds to initial rapid uptake, taking place at under film boundary control and the second line corresponds to intraparticle diffusion under pore geometry control. It is interesting to see that these results of effect of mass transfer on kinetics of adsorption are confirming the high value of activation energy associated with the sorption in section 3.6.
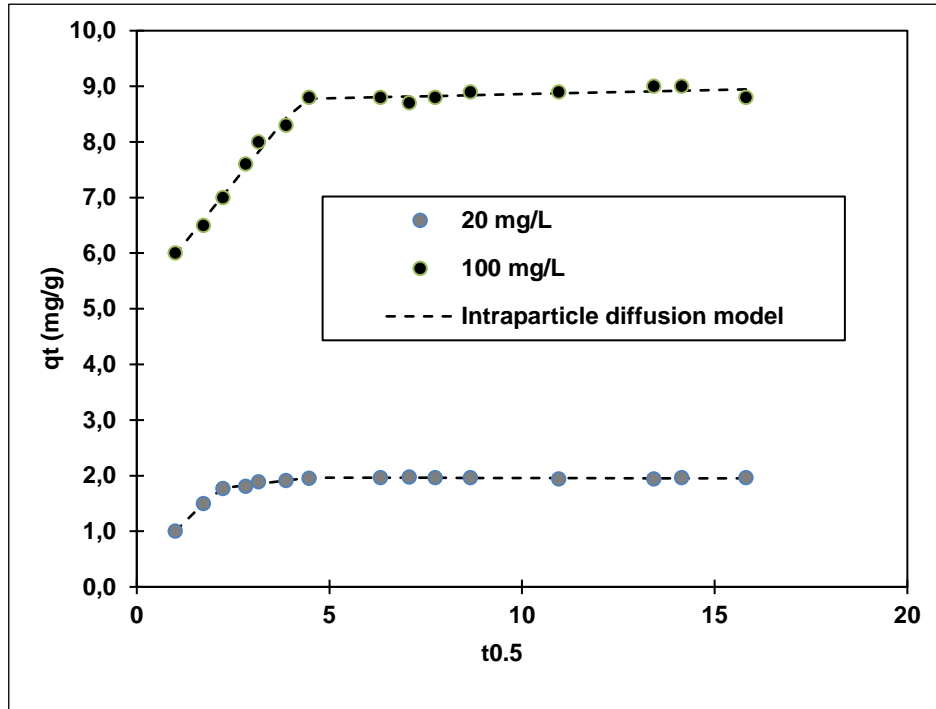

Figure 6–Impact of intraparticle diffusion for Cu(II) sorption onto S-HAP at C_o =20 and 100mg/L.

3.4 Isotherm studies

Conventional isotherm models such as Langmuir, Freundlich and Sips models were used to predict trends of copper uptakes at adsorption equilibrium boundaries. Langmuir model simplifies the sorption into a simple monolayer, containing actives sites of similar state energies [43], and is given by equation (Eq.(4)):

$$q_e = \frac{q_{max}bC_e}{1+bC_e} \tag{4}$$

Where q_e is the equilibrium uptake (mg/g), C_e is the equilibrium concentration (mg/L), q_{max} is the maximum uptake or sorption capacity (mg/g), and b (L/mg) is the Langmuir equilibrium constant.

Alternatively, Freundlich model, which describes general heterogeneous systems, use a semi-empirical expression as expressed by equation (Eg.(5))[43]:

$$q_e = K_F C_e^{1/n} \tag{5}$$

Where K_F (mg$^{1-1/n}$ L$^{1/n}$ g^{-1}) and n are constants which describe sorbent–sorbate interactions. Furthermore, the Sips isotherm model which include features of both mentioned models [44, 45], reduces to the Freundlich isotherm at low concentrations, predicts a Langmuir monolayer sorption capacity at high concentrations and expressed by equation (Eq.(6)):

$$q_e = q_{max}\left[\frac{K_s C_e^{n_s}}{1+K_s C_e^{n_s}}\right] \tag{6}$$

Where K_s and n_s are the Sips parameters and depend on sorbent-sorbate characteristics.

Figures 7a and 7b band and Table 3 show isotherm trends of copper ions on N-HAP and S-HAP, respectively, along with relevant constants.
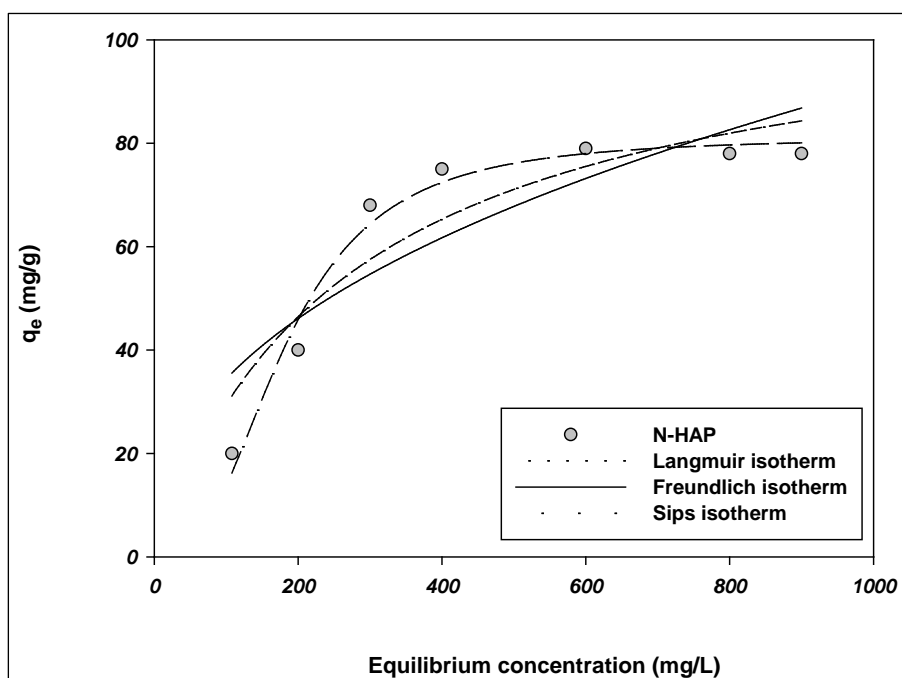

Figure 7a - Adsorption isotherms of Cu(II) on N-HAP at pH 4 and 20°C and contact time of 180 min.
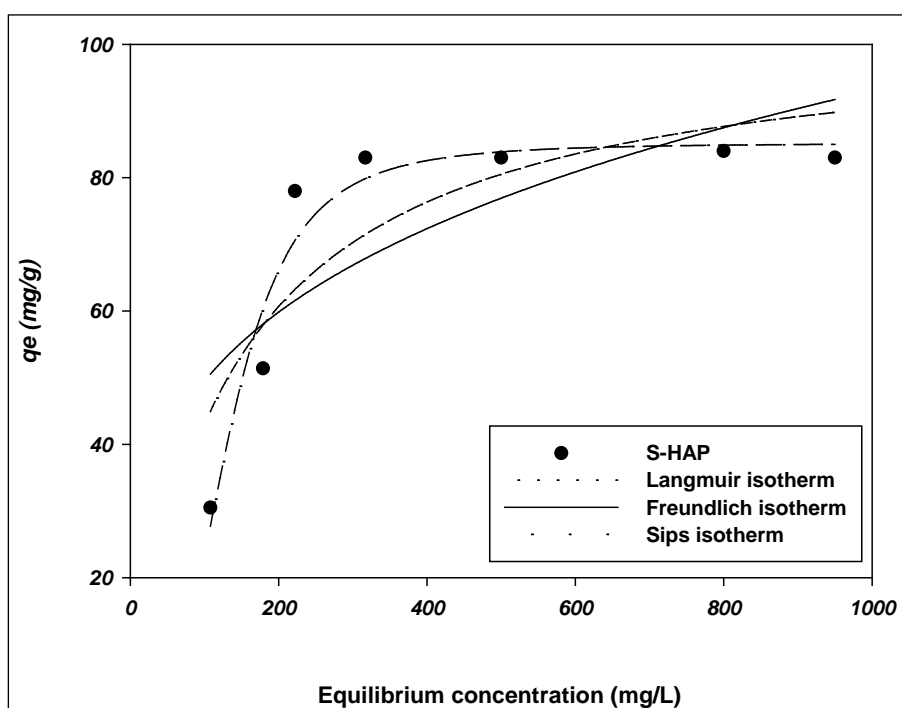

Figure 7b - Adsorption isotherms for Cu(II) on S-HAP at pH 4 and 20°C, and contact time of 180 min.

Sips isotherm offered a better fit of experimental data than Langmuir or Freundlich isotherms. The values of R^2 ranged from 0.757 (S-HAP) to 0.856 (N-HAP) for Langmuir model, from 0.599 (S-HAP) to 0.764 (N-HAP) for Freundlich model, and from 0.941 (S-HAP) to 0.977 (N-HAP) for Sips isotherm. The Sips model is then convenient in case of a chemical heterogeneous sorbent that leads to multiple mechanisms of sorption. It is logical to use the Sips model without any

mathematical limit for its parameters during the data fitting method. The sorption was a complex process due to non-identical binding sites and that was influenced by geometry and chemical affinity between the sorbate and the sorbent [43].

Table 3: Adsorption isotherm constants values.

	Langmuir isotherm model			Freundlich isotherm model			Sips isotherm model			
	q_{max}	b	R^2	K_F	n	R^2	q_{max}	$K_s(10^7)$	n_s	R^2
N-HAP	109.9	0.004	0.856	4.956	2.376	0.764	**81.15**	9.108	2.674	**0.977**
S-HAP	102.9	0.007	0.757	13.98	3.646	0.599	**85.17**	1.544	3.194	**0.941**

The performance of the three models for copper sorption on N-HAP or S-HAP is given by: Sips > Langmuir >Freundlich. Also, the q_{max} values determined by the Langmuir isotherm were 109.9mg/g and 102.9 mg/g of N-HAP and S-HAP, respectively. But on the Sips isotherm model, q_{max}, was found to be 81.15 and 85.17 mg/g for N-HAP and S-HAP respectively. The similar adsorption capacities despite the difference in surface area may be attributed to similar number of active sites available.

Table 4 provides a comparaison among the adsorbents investigated herein and those listed reported in literature.

Table 4: Comparison among the adsorbents investigated herein and those listed in literature about copper removal

Adsorbents	Adsorption capacity (mg/g)	Reference
p(AMPS) hydrogels	100.8	44
Magnetic p(AMPS) composite hydrogels	105.6	44
Natural bentonite	7.9	45
Natural zeolite	8.9	46
Kaolinite	10.7	47
Cellulose	7.0	48
Peanut hull Carbon	65.5	49
Activated Carbon	4.4	50
Pretreated fish bones	150.7	29
N-Hap	109.9*	This Study
S-Hap	102.9*	This Study

*Value Given from Langmuir model

3.5 Adsorption mechanism

In order to suggest a mechanism for copper sorption on N-HAP and S-HAP, the amount calcium released along with copper sorbed at equilibrium conditions was investigated as shown in Figure 8.

FTIR spectra analyses for N-HAP (Figure 9) and S-HAP (Figure 10) before and after sorption of Cu(II) were carried out as well. N-HAP and S-HAP FTIR analysis show absorption bands of hydroxyapatite at 1024 cm^{-1} which indicates phosphate group PO_4^{3-}. The FTIR spectra (Figures 9 and 10) of all samples show bands corresponding to HAP structure, including absorbed water, hydroxyl and phosphate species. Some carbonate derived bands were observed at 876 cm^{-1} and around 1420 and 1458 cm^{-1}. It might be due to the adsorption of atmospheric carbon dioxide during the sample preparation [7, 24, 29, 51-52].
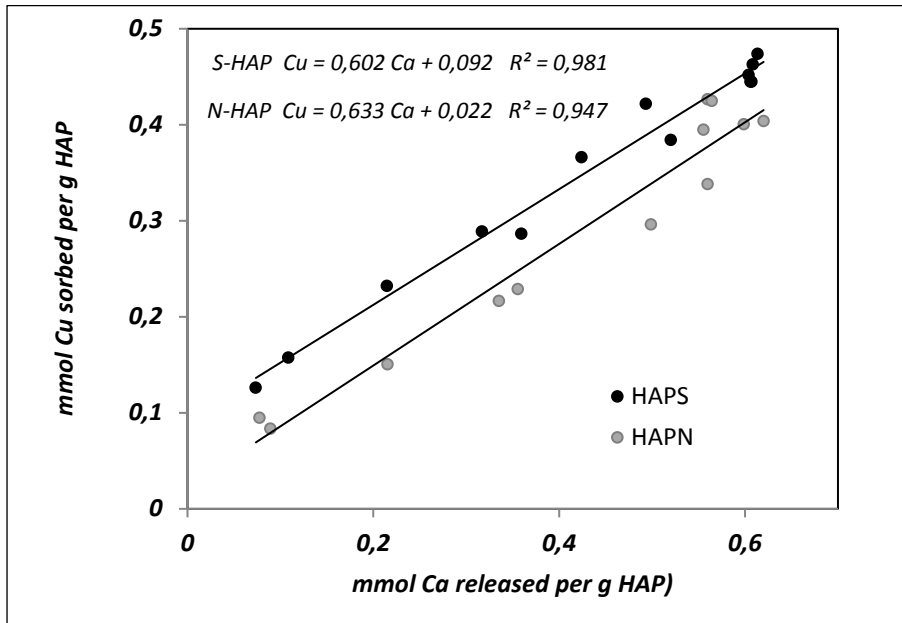
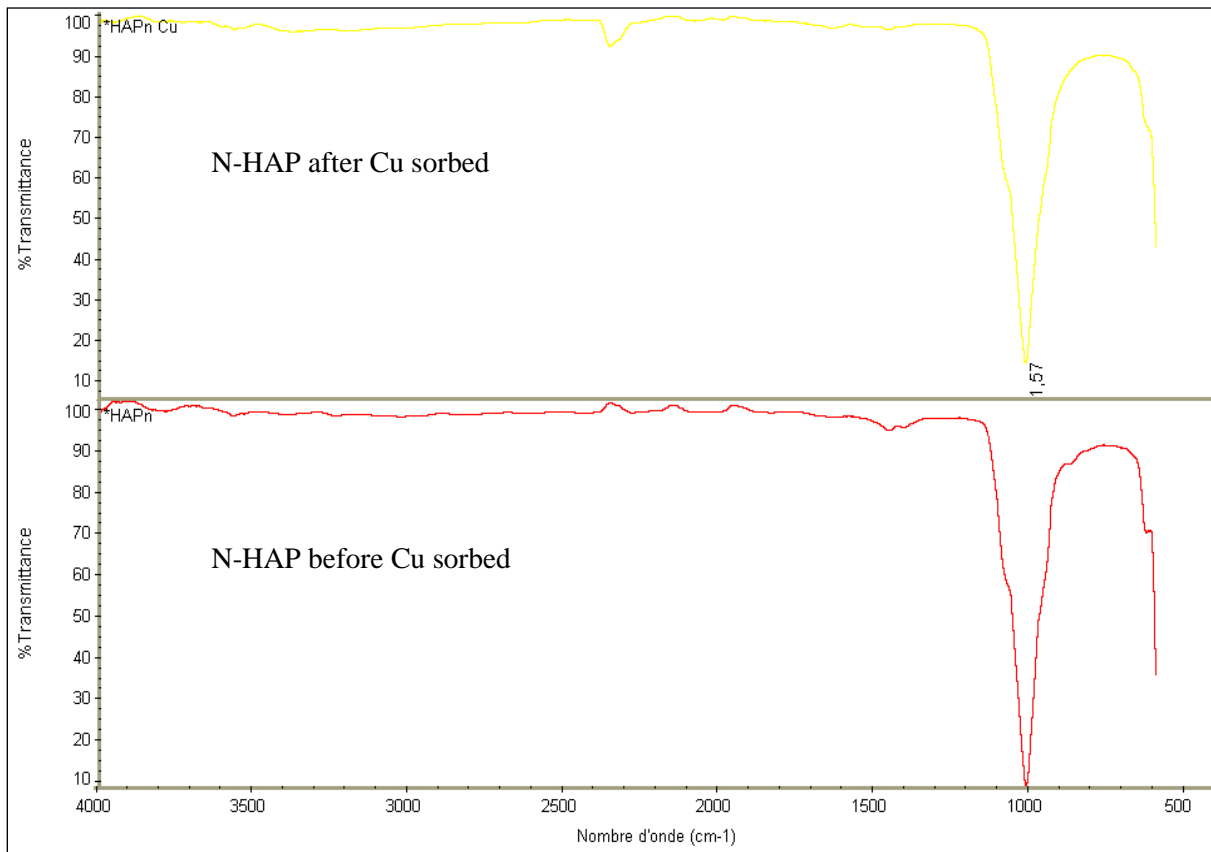*Figure 8- Variation of amount Cu sorbed on apatite as a function of Ca released in solution (20 °C, pH4)*

Figure 9 - FT-IR spectra of N-HAP sorbent before and after 3hours contact with 100ppm Copper solution

The absorption band at about $632 cm^{-1}$ corresponds to the OH^- vibrational mode (Figures 9 and 10). In addition to the broad vibration bands at 1020 and $1080 cm^{-1}$ were attributed to development of HAP [1,7]. The vibration bands with a wide shoulder at $962–1105 cm^{-1}$ were attributed to the P–O stretching of the phosphate groups (PO_4^{3-}). Figure 10 shows nitrates (NO_3^{2-}) band intensity at $1300 cm^{-1}$ and carbonates (CO_3^{2-}) at $1430 cm^{-1}$ (FTIR Spectra of S-HAP before Cu sorbed) which disappear when Cu (II) was adsorbed onto the surface of S-HAP (FTIR Spectra of S-HAP after Cu sorbed).
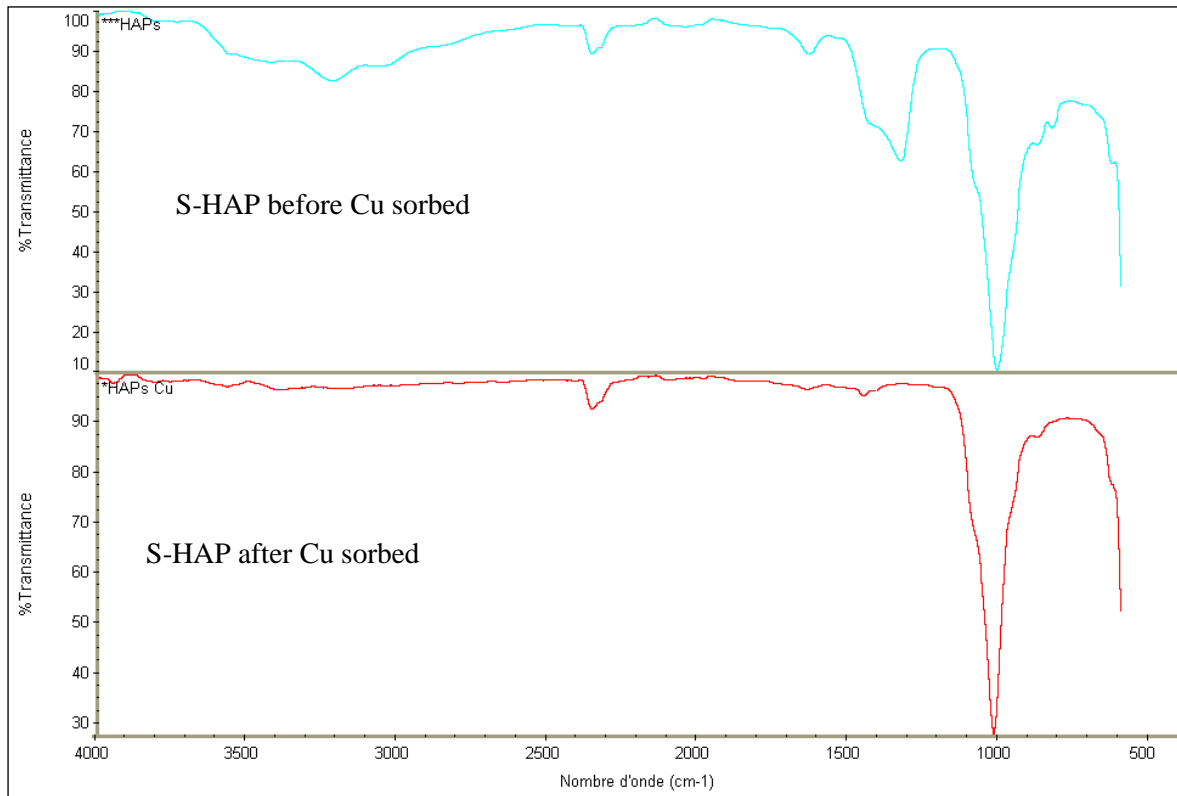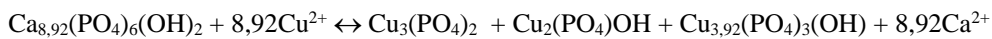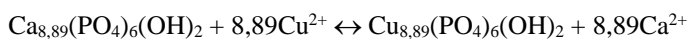
Figure 10 - FT-IR spectra of S-HAP sorbent before and after 3hours contact with 100ppm Copper solution

The removal of Cu ions by hydroxyapatite has been recurrently interpreted by a single sorption but also by combined process of sorption, dissolution of sorbent and precipitation of both amorphous copper phosphates ($Cu_3(PO_4)_2$) and libethenite ($Cu_2(PO_4)OH$) [7, 24-25, 37, 51-52]. However, on the basis of SEM, FTIR and Figure 8 results we can consider the following reactions as responsible of Cu(II) sorption mechanism on N-HAP and S-HAP:

<u>For N-HAP</u>: Partial ion exchange between Ca^{2+} and Cu^{2+} and precipitation of amorphous copper phosphates ($Cu_3(PO_4)_2$) and libethenite ($Cu_2(PO_4)OH$) :

$Ca_{8,92}(PO_4)_6(OH)_2 + 8,92Cu^{2+} \leftrightarrow Cu_3(PO_4)_2 + Cu_2(PO_4)OH + Cu_{3,92}(PO_4)_3(OH) + 8,92Ca^{2+}$

<u>For S-HAP</u>: Ion exchange between Ca^{2+} and Cu^{2+}

$Ca_{8,89}(PO_4)_6(OH)_2 + 8,89Cu^{2+} \leftrightarrow Cu_{8,89}(PO_4)_6(OH)_2 + 8,89Ca^{2+}$

3.6 Thermodynamic parameters

Since the two HAPs presented similar trends, impact of temperature on kinetics of adsorption of copper ions onto S-HAP was investigated as shown in Figure 11. Temperature is anticipated to affect both the rate and extent of sorption and thus would provide information on potential underlying mechanism [6].

The adsorption capacity for copper increased from 79.19 mg/g to 97.84mg/g when temperature increased from 20°C to 60°C. Temperature stimulated both $Cu^{2+}$the boundary layer diffusion and sorption, demonstrating an endothermic nature of the process [1, 6]. The adsorption data at different values of temperature were used to estimate thermodynamic state functions, accompanying the sorption such as enthalpy change (ΔH), Gibbs free energy change (ΔG) and entropy change (ΔS) expressed by Eqs. (7) to (9) [31,42]:

$$\Delta G = -RT \ln k_c \qquad (7)$$

$$\Delta G = \Delta H - T\Delta S \qquad (8)$$

$$\ln k_c = \frac{\Delta S}{R} - \frac{\Delta H}{R}\frac{1}{T} \qquad (9)$$

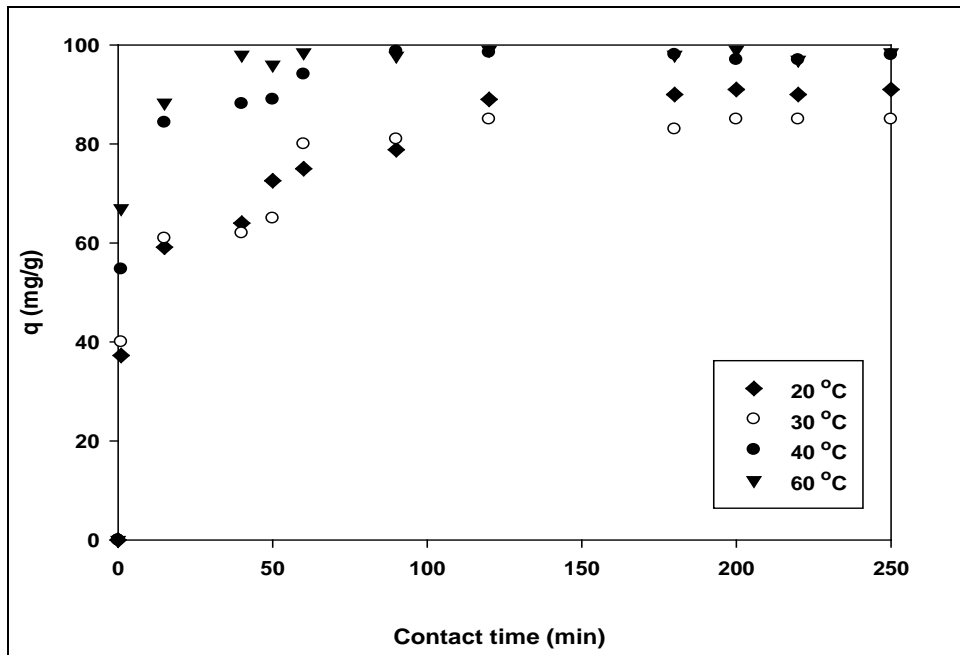Where R is the universal gas constant (8.314 J/mol K) and k_c is the adsorption equilibrium constant.

Figure 11 -Effect of temperature on copper removal on S-HAP (1000ppm, 10 g HAP/L, pH 4).

A linear plot of ln$k$ *versus* $1/T$ shown in Figure 12 was used to find the values of enthalpy and entropy changes (i.e. 74.64 kJ/mol and 260.72 kJ/mol.K, respectively). Gibbs free energy, as illustrated in Table 5, shows negative values at all temperatures, indicating that the adsorption process was spontaneous and favourable while the positive values of ΔH and ΔS confirm the natural endothermicity of copper sorption and the increased randomness at the solid-solution boundary. Such increase was likely driven by water molecules which were transferred the adsorbate species, gaining more translational entropy than ions lost by later species [43].

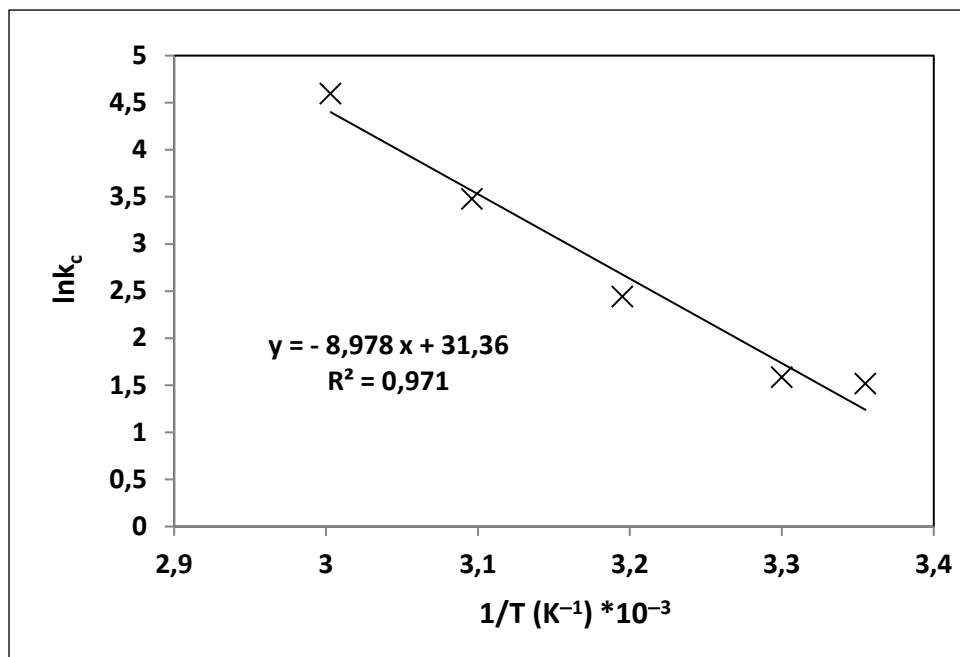$$y = -8,978 x + 31,36$$
$$R^2 = 0,971$$

Figure 12. Van't Hoff plot for different solution temperatures for copper removal using S-HAP (S-HAP amount=0.5 g, pH=4, copper concentration=1000 ppm, copper solution volume=50 ml, agitation speed=600 rpm)

Table 5: The Gibbs free energy change ΔG for different solution temperature of copper removal using S-HAP

Temperature (K)	ΔG (kJ/mol)
293	− 3,756
303	− 3,994
313	− 6,356
323	− 9,335
333	− 12,722

4 Conclusion

The advantages of hydroxyapatites, including affordability, availability, natural origin and high adsorption capacity, are driving these materials to be attractive as sorbents to reduce toxic metals. The results of batch operations removal of copper ions from aqueous solutions by sorption were efficient on both S-HAP and N-HAP sorbents. The obtained data copper adsorption fitted well Sips -type isotherms compared to conventional Langmuir and Freundlich isotherms. The values obtained for maximum uptake confirmed that HAP presents favourable sorption efficiency towards copper ions. These properties would direct to interesting applications to water treatments. Based on the Sips isotherm model, the predicted maximum capacity of adsorbent was found to be 81,15 and 85,17 mg/g for N-HAP (1,5 m^2/g) and S-HAP (43,16m^2/g) respectively. Thus Cu sorption level per square meter is 54,1 mg/m^2 and 1,97mg/m^2 for N-HAP and S-HAP, respectly. These results show that for the same contact surface N-HAP is 27 times more effective than S-HAP with respect sorption Cu ions in solution. In an industrial scale to treat 100m^3 of water containing 1000ppm Cu (II) the estimated amount of Hydroxyapatite is about 1200 kG. Furthermore the cost price of natural and synthetic hydroxyapatite is less expensive compared to another adsorbent such as activated carbon for example.

The present study clearly revealed that natural and synthetic hydroxyapatite can be used for processing industrial wastes containing toxic metal ions. In addition, the rate of sorption was found weakly affected by intra-particle diffusion which would benefit the design of packed beds holding beads of particles of large size and reduced pressure drops. The performance of sorption was however affected by parameters such as: solution temperature, amount of HAP and initial copper concentration ratio, requiring suitable design parameters for industrial scale up. Sorption of Cu(II) on N-HAP and S-HAP is better fitted by the pseudo-first order kinetic model based on the assumption of ion-exchange associated the sorption and played a non-negligible role in the overall kinetic mechanism.

REFERENCES

[1]- W. Zheng, X.-M. Li, Q. Yang, G.-M. Zeng, X.-X. Shen, J.-J. Liu, Y. Zhang, Adsorption of Cd(II) and Cu(II) from aqueous solution by carbonate hydroxylapatite derived from eggshell waste. J. Hazard. Mater. 147(1-2) (2007) 534–539. doi:10.1016/j.jhazmat.2007.01.048

[2]- S.E. Bailey, T.J. Olin, R.M. Bricka, D.D. Adrian, A review of potentially low-cost sorbents for heavy metals. Water Res. 33(11) (1999) 2469-2479. doi:10.1016/S0043-1354(98)00475-8

[3]- C.W. Cheung, J.F. Porter, G. Mckay, Sorption kinetic analysis for the removal of cadmium ions from effluents using bone char. Water Res. 35(3) (2001) 605-612. doi:10.1016/S0043-1354(00)00306-7

[4]- U.S. Department of Health and Human Services, Toxicological Profile for Cadmium. In: Agency for Toxic Substances and Disease Registry, 1999.

[5]- S.S. Gupta, K.G. Bhattacharyya, Removal of Cd(II) from aqueous solution by kaolinite, montmorillonite and their poly(oxo zirconium) and tetrabutylammonium derivatives. J. Hazard. Mater. 128(2-3) (2006) 247-257. doi:10.1016/j.jhazmat.2005.08.008

[6]- M.F. Elkady, M.M. Mahmoud, H.M. Abd-El-Rahman, Kinetic approach for cadmium sorption using microwave

synthesized nano-hydroxyapatite. J. Non-Cryst. Solids 357(3) (2011) 1118–1129. doi:10.1016/j.jnoncrysol.2010.10.021

[7]- M. Šljivić, I. Smičiklas, I. Plećaš, M. Mitrić, The influence of equilibration conditions and hydroxyapatite physico-chemical properties onto retention of Cu^{2+} ions. Chem. Eng. J. 148 (2009) 80-88. doi:10.1016/j.cej.2008.08.003

[8]- A.H. Mahvi, A. Maleki, A. Eslami, Potential of Rice Husk and Rice Husk Ash for Phenol Removal in Aqueous Systems. Am. J. Appl. Sci. 1(4) (2004) 321-326.

[9]- A. Duffy, G.M. Walker, S.J. Allen, Investigations on the adsorption of acidic gases using activated dolomite. Chem. Eng. J. 117(3) (2006) 239-244. doi:10.1016/j.cej.2005.11.016

[10]- A.B. Albadarin, C. Mangwandi, G.M. Walker, S.J. Allen, M.N. Ahmad, Biosorption characteristics of sawdust for the removal of Cd(II) ions: mechanism and thermodynamic studies. Chem. Engineer. Trans. 24(2011) 1297–1302. doi:10.3303/CET1124217

[11]- I. Villaescusa, N. Fiol, M. Martínez, N. Miralles, J. Poch, J. Serarols, Removal of copper and nickel ions from aqueous solutions by grape stalks wastes. Water Res. 38(4) (2004) 992-1002. doi:10.1016/j.watres.2003.10.040

[12]- A. Saeed, M. Iqbal, M.W. Akhtar, Removal and recovery of lead(II) from single and multimetal (Cd, Cu, Ni, Zn) solutions by crop milling waste (black gram husk). J. Hazard. Mater. 117(1) (2005) 65-73. doi:10.1016/j.jhazmat.2004.09.008

[13]- N. Fiol, I. Villaescusa, M. Martínez, N. Miralles, J. Poch, J. Serarols, Sorption of Pb(II), Ni(II), Cu(II) and Cd(II) from aqueous solution by olive stone waste. Sep. Purif. Technol. 50(1) (2006) 132-140. doi:10.1016/j.seppur.2005.11.016

[14]- F. Monteil-Rivera, M. Fedoroff, Sorption of inorganic species on apatites from aqueous solutions. In: Encyclopedia of Surface and Colloid Science, Ed. P. Somasundaran, 2001, pp.1-26.

[15]- J.A. Gómez del Río, P.J. Morando, D.S. Cicerone, Natural materials for treatment of industrial effluents: comparative study of the retention of Cd, Zn and Co by calcite and hydroxyapatite. Part I: batch experiments. J. Environ. Manage. 71(12) (2004) 169-177. doi:10.1016/j.jenvman.2004.02.004

[16]- M. Peld, K. Tõnsuaadu, V. Bender, Sorption and desorption of Cd^{2+} and Zn^{2+} ions in apatite-aqueous systems. Environ. Sci. Technol. 38 (2004) 5626-5631. doi:10.1021/es049831l

[17]- B.M. Thomson, C.L. Smith, R.D. Busch, M. Siegel, C. Baldwin, Removal of Metals and Radionuclides Using Apatite and Other Natural Sorbents. J. Environ. Eng. 129(6) (2003) 492–499. doi:10.1061/(ASCE)0733-9372(2003)129:6(492)

[18]- M. Mouflih, A. Aklil, S. Sebti, Removal of lead from aqueous solutions by activated phosphate. J. Hazard. Mater., 119(1-3) (2005) 183-188. doi:10.1016/j.jhazmat.2004.12.005

[19]- S. McGrellis, J.N. Serafini, J. JeanJean, J.-L. Pastol, M. Fedoroff, Influence of the sorption protocol on the uptake of cadmium ions in calcium hydroxyapatite. Sep. Purif. Technol. 24(1-2) (2001) 129-138. doi:10.1016/S1383-5866(00)00223-9

[20]- D.C.K. Ko, C.W. Cheung, K.K.H. Choy, J.F. Porter, G. McKay, Sorption equilibria of metal ions on bone char. Chemosphere 54(3) (2004) 273-281. doi:10.1016/j.chemosphere.2003.08.004

[21]- Y.S. Ho, G. McKay, Pseudo-second order model for sorption processes. Process Biochem. 34(5) (1999) 451-465. doi:10.1016/S0032-9592(98)00112-5

[22]- J.L. Conca, J. Wright, An Apatite II permeable reactive barrier to remediate groundwater containing Zn, Pb and Cd. Appl. Geochem. 21(8) (2006) 1288-1300. doi:10.1016/j.apgeochem.2006.06.008

[23]- M.E. Hodson, É. Valsami-Jones, J.D. Cotter-Howells, Bonemeal additions as a remediation treatment for metal contaminated soil. Environ. Sci. Technol. 34(2000) 3501-3507. doi:10.1021/es990972a

[24]- A. Corami, F. D'Acapito, S. Mignardi, V. Ferrini, Removal of Cu from aqueous solutions by synthetic hydroxyapatite: EXAFS investigation. Mater. Sci. Eng. B 146(2) (2008) 209-2013. doi:10.1016/j.mseb.2007.11.006

[25]- A. Corami, S. Mignardi, V. Ferrini, Copper and zinc decontamination from single- and binary-metal solutions using hydroxyapatite, J. Hazard. Mater. 146(1-2) (2007) 164-170. doi:10.1016/j.jhazmat.2006.12.003

[26]- I. Smičiklas, A. Onjia, S. Raičević, Đ. Janaćković, M. Mitrić, Factors influencing the removal of divalent cations by hydroxyapatite. J. Hazard. Mater. 152(2) (2008) 876-884. doi:10.1016/j.jhazmat.2007.07.056

[27]- F. Fernane, M.O. Mecherri, P. Sharrock, M. Hadioui, H. Lounici, M. Fedoroff, Sorption of cadmium and copper ions on natural and synthetic hydroxylapatite particles. Mater. Charact. 59(5) (2008) 554-559. doi:10.1016/j.matchar.2007.04.009

[28]- F. Fernane, M.O. Mecherri, P. Sharrock, M. Fiallo, R. Sipos, Hydroxyapatite interactions with copper complexes.

Mater. Sci. Eng.-C 30(7) (2010) 1060-1064. doi:10.1016/j.msec.2010.05.010

[29]- B. Kizilkaya, A.A. Tekinay, Y. Dilgin, Adsorption and removal of Cu (II) ions from aqueous solution using pretreated fish bones. Desalination 264(1-2) (2010) 37-47. doi:10.1016/j.desal.2010.06.076

[30]- S. Sugiyama, T. Ichii, M. Fujisawa, K. Kawashiro, T. Tomida, N. Shigemoto, H. Hayashi, Heavy metal immobilization in aqueous solution using calcium phosphate and calcium hydrogen phosphates. J. Colloid Interf. Sci. 259(2) (2003) 408-410. doi:10.1016/S0021-9797(02)00211-4

[31]- Z. Elouear, J. Bouzid, N. Boujelben, M. Feki, F. Jamoussi, A. Montiel, Heavy metal removal from aqueous solutions by activated phosphate rock. J. Hazard. Mater. 156(1-3) (2008) 412-420. doi:10.1016/j.jhazmat.2007.12.036

[32]- K. Valsami-Jones, K.V. Ragnarsdottir, A. Putnis, D. Bosbach, A.J. Kemp, G. Gressey, The dissolution of apatite in the presence of aqueous metal cations at pH 2–7. Chem. Geol. 151(1-4) (1998) 215–233. doi:10.1016/S0009-2541(98)00081-3

[33]- J. Oliva, J. De Pablo, J.-L. Cortina, J. Cama, C. Ayora, Removal of cadmium, copper, nickel, cobalt and mercury from water by Apatite II™: Column experiments. J. Hazard. Mater. 194 (2011) 312-323. doi:10.1016/j.jhazmat.2011.07.104

[34]- F.D. Tillman Jr, S.L. Bartelt-Hunt, J.A. Smith, G.R. Alther, Evaluation of an Organoclay, an Organoclay-Anthracite Blend, Clinoptilolite, and Hydroxy-Apatite as Sorbents for Heavy Metal Removal from Water. B. Environ. Contam. Tox. 72 (2004) 1134–1141. doi:10.1007/s00128-004-0362-8

[35]- E.-S. Bogya, I. Bâldea, R. Barabás, A. Csavdári, G. Turdean, V.-R. Dejeu, Kinetic studies of sorption of copper(ii) ions onto Different calcium-hydroxyapatie materials. Stud. U Babes-Bol. Chem. 45(2) (2010).

[36]- A. Jurkiewicz, D. Wiechuła, R. Nowak, T. Gaździk, K. Loska, Metal content in femoral head spongious bone of people living in regions of different degrees of environmental pollution in Southern and Middle Poland. Ecotox. Environ. Safe. 59 (2004) 95-101. doi:10.1016/j.ecoenv.2004.01.002

[37]- F. Fernane, S. Boudia, F. Aiouache, Removal Cu(II) and Ni(II) by natural and synthetic hydroxyapatites : a comparative study. Desalin. Water Treat. 52(13-15) (2014) 2856 −2862. doi:10.1080/19443994.2013.807084

[38]- S. Elfersi, G. Grégoire, P. Sharrock, Characterization of sound human dentin particles of sub-millimeter size. Dent. Mater. 18(7) (2002) 529-534. doi:10.1016/s0109-5641(01)00085-9

[39]- Q. Fan, D. Shao, Y. Lu, W. Wu, X. Wang, Effect of pH, ionic strength, temperature and humic substances on the sorption of Ni(II) to Na–attapulgite. Chem. Eng. J. 150(1) (2009) 188-195. doi:10.1016/j.cej.2008.12.024

[40]- B.H. Hameed, M.I. El-Khaiary, Malachite green adsorption by rattan sawdust: Isotherm, kinetic and mechanism modeling. J. Hazard. Mater. 159(2-3) (2008) 574-579. doi:10.1016/j.jhazmat.2008.02.054

[41]- A.B. Albadarin, J. Mo, Y. Glocheux, S. Allen, G. Walker, C. Mangwandi, Preliminary investigation of mixed adsorbents for the removal of copper and methylene blue from aqueous solutions. Chem. Eng. J. 255 (2014) 525-534. doi:10.1016/j.cej.2014.06.029

[42]- A.B. Albadarin, C. Mangwandi, G.M. Walker, S.J. Allen, M.N.M. Ahmad, M. Khraisheh, Influence of solution chemistry on Cr(VI) reduction and complexation onto date-pits/tea-waste biomaterials. J. Environ. Manage. 114(2013) 190-201. doi:10.1016/j.jenvman.2012.09.017

[43]- A.B. Albadarin, C.Mangwandi, A. Al-Muhtaseb, G.M. Walker, S.J. Allen, M. N.M. Ahmad, Kinetic and thermodynamics of chromium ions adsorption onto low-cost dolomite adsorbent. Chem. Eng. J. 179 (2012) 193–202. doi:10.1016/j.cej.2011.10.080

[44]- O. Ozay, S. Ekici, Y. Barana, N. Aktas, N. Sahiner, Removal of toxic metal ions with magnetic hydrogels. Water Res. 43(17) (2009) 4403–4411. doi:10.1016/j.watres.2009.06.058

[45]- N. Karapinar, R. Donat, Adsorption behaviour of Cu^{2+} and Cd^{2+} onto natural bentonite. Desalination 249(1) (2009) 123–129. doi:10.1016/j.desal.2008.12.046

[46]- E. Erdem, N. Karapinar, R. Donat, The removal of heavy metal cations by natural zeolites. J. Colloid Interf. Sci. 280(2) (2004) 309–314. doi:10.1016/j.jcis.2004.08.028

[47]- O. Yavuz, Y. Altunkaynak, F. Guzel, Removal of copper, nickel, cobalt and manganese from   aqueous solution by kaolinite. Water Res. 37(4) (2003) 948–952. doi:10.1016/S0043-1354(02)00409-8

[48]- B. Acemioglu, M.H. Alma, Equilibrium studies on adsorption of Cu(II) from aqueous solution onto cellulose. J. Colloid Interf. Sci. 243(1) (2001) 81–84. doi:10.1006/jcis.2001.7873

[49]- K. Periasamy, C. Namasivayam, Removal of copper(II) by adsorption onto peanut hull carbon from water and copper plating industry wastewater. Chemosphere 32(4) (1996) 769–789. doi:10.1016/0045-6535(95)00332-0

[50]- K.H. Chu, M.A. Hashim, Adsorption of copper(II) and EDTA-chelated copper(II) onto granular activated carbons.

J. Chem. Technol. Biot. 75(11) (2000) 1054–1060. doi:10.1002/1097-4660(200011)75:11<1054::AID-JCTB315>3.0.CO;2-T

[51]- Å. Bengtsson, S. Sjöberg, Surface complexation and proton-promoted dissolution in aqueous apatite systems. Pure Appl. Chem. 81(9) (2009) 1569–1584. doi:10.1351/PAC-CON-08-10-02

[52]- K. Viipsi, S. Sjöberg, A. Shchukarev, K. Tõnsuaadu, Surface phase transformations, surface complexation and solubilities of hydroxyapatite in the absence/presence of Cd(II) and EDTA. Appl. Geochem. 27(2012) 15–21. doi:10.1016/j.apgeochem.2011.08.010